Available online at www.sciencedirect.com
SCIENCE DIRECT®
Polymer 45 (2004) 133–140
polymer
www.elsevier.com/locate/polymer

Polymeric amine bearing side-chain thioxanthone as a novel photoinitiator for photopolymerization

Xuesong Jiang, Hongjie Xu, Jie Yin*

State Key Laboratory for Composite Materials, School of Chemistry and Chemical Technology, Research Institute of Polymer Materials, Shanghai Jiao Tong University, Shanghai 200240, People's Republic of China

Received 7 June 2003; received in revised form 6 October 2003; accepted 22 October 2003

Abstract

Novel polymeric photoinitator (PTX) was synthesized by introducing thioxanthone (TX) moieties to polymeric amine side-chain. Compared with low-mulecular weight model compound, PTX has similar UV–vis absorption and weaker fluorescence emission, and some radicals are trapped in the macromolecular coil cage. The kinetics for polymerization of trimethylolpropane triacrylate using PTX as photoinitiator was studied by photo-DSC. It shows that PTX is an efficient photoinitiator, and that PTX concentration and light intensity have similar effect on photopolymerization. The increase in PTX concentration and light intensity leads to the increase in the polymerization rate and the final conversion. The increase in temperature also results in the increase in the polymerization rate and final conversion, due to the enhanced molecular mobility and delay in vitrification at high temperature. At the late stage of polymerization, the reaction becomes more diffusion-controlled than that at early stage of polymerization.

Keywords: Polymeric photoinitiator; Thioxanthone; Photopolymerization

1. Introduction

Photopolymerization science and technology have assumed in recent years an increasing relevance in many applications, such as curing of coatings on various materials, adhesives, printing inks, and photoresists [1]. This technology is based on the use of photoinitiator systems suited to absorb a light radiation of the appropriate wavelength and to produce primary radical species able to convert a multifunctional monomer into a cross-linked network. Among the most studied photoinitiator systems are those in which radicals are formed by a bimolecular process consisting of an excited chromophore and an amine as a coinitiator [2–5]. Polymeric photoinitiator systems, which can be prepared by introducing chromophore and amine into polymer chains, have obvious advantages such as good solubility and compatibility in the curable medium, low odor and toxicity, due to the well-known polymer effect [6–10]. In particular, an improvement in photoinitiation activity can be obtained as the result of energy migration between excited- and ground-state photosensitive moieties along the polymer chain or of intramolecular reactions affording more reactive species which can be protected as in a cage by the microenvironment of the polymer chains, thus reducing their tendency to coupling processes [8].

The other important research field in photopolymerization is the polymerization kinetics of multifunctional monomers which determines the structure and physical properties of final polymer networks. This has been the subject of many investigations [11–20], which have shown that the photopolymerization of multifunctional monomers can exhibit unique reaction behavior including unequal functional group reactivity and auto-acceleration induced by diffusion-controlled propagation and termination.

In this context, taking into account that thioxanthone derivatives in conjunction with amines are efficient photoinitiators [3,7,21–25], we synthesized polymeric photoinitiator by introducing thioxanthone moieties into poly(ethylene imine) (PEI) side-chain, as well as low weight molecular model compound, purposely prepared to compare the properties of the low and high molecular weight photoinitiators, and then studied the kinetics for

* Corresponding author. Tel.: +86-21-5474-6215; fax: +86-21-54741-297.
E-mail address: jyin@sjtu.edu.cn (J. Yin).

0032-3861/$ - see front matter © 2003 Elsevier Ltd. All rights reserved.
doi:10.1016/j.polymer.2003.10.058

polymerization of trimethylolpropane triacrylate (TMPTA), which is common by used multifuncational acrylates, by photo differential scanning calorimetry (photo-DSC).

2. Experimental

2.1. Materials

Thiosalicylic acid (from Fluka), PEI (M_w 2500, from BDH), TMPTA (from Nantong Litian chemical company) were used as received. Other chemicals are of analytical grade except as noted. Epichlorohydrin was purified by refluxing with calcium hydroxide and redistilled.

2.2. Synthesis

2.2.1. Preparation of polymeric photoinitiator (PTX)

A mixture of 1.0 g of 2-(2,3-epoxy)propoxylthioxanthone (synthesized according to Ref. [27]), 1.5 g of poly(ethylene imine), 40 ml of ethanol was stirred at 80 °C for 10 h, and then filtered through a thin layer of activated charcoal after cooling. The filtrate was evaporated to remove ethanol, and residue was dissolved in water and washed with benzene in a separating funnel. The aqueous layer was separated and water was evaporated and the residue was re-dissolved in ethanol, which was then precipitated in 10-fold excess ether and dried in vacuo to obtain the polymeric photoinitiator.

UV: $\lambda = 398$ nm $\log \varepsilon = 3.74$. ^{1}H NMR (400 MHz) in $CDCl_3$: 8.67–8.42 (1H, aromatic), 8.15–7.91 (1H, aromatic), 7.64–7.25 (5H, aromatic), 4.01–4.05 (2H OCH_2), 3.85 (1H OCH), 2.05–3.05 (52H NCH_2, OH and NH). FT-IR (KBr):1634 (C=O), 2815, 2944 (C–H), 3360–3500 (N–H, O–H). Elemental analysis, found: C, 49.13%; H, 9.85%; N, 15.99%; S, 3.54%. T_g (DSC in N_2, 10 °C/min): −20.3 °C.

2.2.2. Preparation of model compound ATX

A mixture of 1.0 g of 2-(2,3-epoxy)propoxylthioxanthone, 2 ml of diethylamine (DEA), 40 ml of ethanol was stirred at 80 °C for 4 h, and then filtered through a thin layer of activated charcoal after cooling. The filtrate was evaporated to remove ethanol and unreacted diethylamine, and the residue was dissolved in diluted hydrochloric acid and washed with benzene in a separating funnel. Ammonia was used to adjust the pH value of the aqueous layer to 8–9, and the solution was extracted with chloroform. The chloroform solution was evaporated to give crude product, which was then recrystallized from mixed solvent of ethanol and water.

UV: $\lambda = 398$ nm $\log \varepsilon = 3.79$. ^{1}H NMR (400 MHz) in $CDCl_3$: 8.67–8.42 (1H, aromatic), 8.15–7.91 (1H, aromatic), 7.64–7.25 (5H, aromatic), 4.11–4.15 (3H OCH_2, OCH), 2.65–2.85 (6H NCH_2), 1.10–1.13 (6H, CH_3). FT-IR (KBr):1636 (C=O), 2815, 2944 (C–H), 3360–3500 (N–H, O–H). Melting point (DSC in N_2): 115 °C. Elemental analysis, calcd for $C_{19}H_{19}NO_3S$: C, 66.86%; H, 5.57%; N, 4.11%; S, 9.38%. Found: C, 66.78%; H, 5.63%; N, 4.09%; S, 9.35%.

2.3. Measurement

The concentration of polymeric photoinitator (PTX) system is in terms of TX moieties and the molar ratio of ATX/DEA in the low-molecular weight photoinitiator systems is always 1:9 in measurement.

2.3.1. Physicochemical measurements

^{1}H NMR spectra were recorded on a Mercury Plus 400 Hz spectrometer with $CDCl_3$ as solvent. FT-IR spectra were recorded on a Perkin–Elmer Paragon1000 FTIR spectrometer. The samples were prepared either as cast films on KBr discs or as KBr pellets. Elemental analysis was conducted on an Elementar Varioel apparatus. Differential scanning calorimetry (DSC) was conducted with a Pyris 1 DSC. UV–vis spectra were recorded in ethanol solution by Perkin–Elmer Lambda 20 UV–vis spectrophotometer. The molar extinction coefficient values ε are expressed as $l\,mol^{-1}\,cm^{-1}$. Fluorescence spectra were recorded in ethanol solution by Perkin–Elmer LS50B luminescence spectrophotometer. ESR experiments were carried out with a Bruker EMX EPR spectrometer at 9.5 GHz with a modulation frequency of 200 kHz with 5,5-dimethyl-1-pyrroline-*N*-oxide (DMPO) as radical capturing agent. A high pressure mercury lamp with a cut-off filter (365 nm) was used for irradiation in the ESR spectrometer cavity. Both concentrations of PTX and ATX dissolved in dichloromethane were 1×10^{-4} M. 0.5 ml of each sample was transformed into a quartz ESR tube and then purged with nitrogen to get rid of oxygen.

2.3.2. Photocalorimetry

The photopolymerization of TMPTA was carried out by DSC 6200 (Seiko Instrument Inc) photo-DSC with incident light of 365 nm, whose intensity can be changed from 5 to 75 mw. Approximately 2 mg sample mixture was placed in the aluminum DSC pans.

Heat flow versus time (DSC thermogram) curves were recorded in an isothermal mode under a nitrogen flow of 50 ml/min. The reaction heat liberated in the polymerization was directly proportional to the number of vinyl groups reacted in the system. By integrating the area under the exothermic peak, the conversion of the vinyl groups (C) or the extent of reaction could be determined according to:

$$C = \Delta H_t / \Delta H_0^{\text{theor}} \quad (1)$$

Where ΔH_t is the reaction heat evolved at time t, and $\Delta H_0^{\text{theor}}$ is the theoretical heat for complete conversion. For an acrylic double bond, $\Delta H_0^{\text{theor}} = 86$ kJ/mol [26]. The rate of polymerization (R_p) is directly related to the heat flow

(dH/dt) by the following equation:

$$R_p = dC/dt = (dH/dt)/\Delta H_0^{theor} \quad (2)$$

3. Results and discussion

3.1. Synthesis of PTX and ATX

PTX and ATX were synthesized by a modified literature [27] procedure described for synthesis of amino-linked thioxanthone according to Scheme 1. The structure of the polymeric photoinitiator and model compound was confirmed by FT-IR and ^{1}H NMR. The PTX composition was determined by the elemental analysis data (nitrogen content/sulfur content). The analysis results showed that the structure unit of PTX *n*/*m* is about 1:9.

3.2. Properties of PTX and ATX/DEA

3.2.1. UV–vis absorption and fluorescence of PTX and ATX/DEA

UV–vis absorption spectra of PTX and ATX/DEA in ethanol are showed in Fig. 1. They exhibit the usual characteristic of absorption of thioxanthone. PTX possesses an absorption similar to ATX/DEA, which shows that macromolecular structure has not obvious influence on UV–vis absorption of thioxanthone moities of PTX.

Although, PTX possesses an emission characteristics similar to ATX/DEA with a maximum at 475 nm, the emission of PTX is obviously weaker than that of ATX/DEA according to the Fig. 2. The weaker emission of PTX can be ascribed to the intramolecular quenching of the aromatic ketone by the amino groups of backbone chains. Compared with ATX, the local amino concentration is larger and the excited TX moieties can be more effectively quenched in the polymeric photoinitiator.

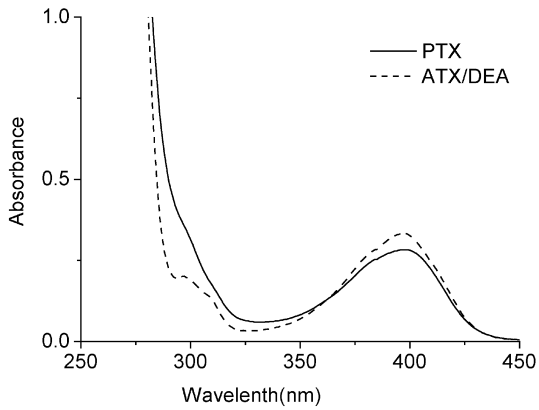

Fig. 1. UV–vis absorption spectra of PTX and ATX/DEA in ethanol solution (PTX = 6×10^{-5} M, ATX = 6×10^{-5} M).

3.2.2. ESR spectroscopy

Spinning-trapping experiments with DMPO were performed to trap amine radicals formed upon irradiation (see Scheme 2). Fig. 3 shows that ESR signals obtained had six-line spectrum, which is explained by a triplet with α-nitrogen and a further split into a doublet with a β-proton. The value of the magnetic parameter, factor-g, was 2.0050, thus indicating that the amine radicals had been released and trapped by DMPO. Compared with that of ATX/DEA, however, the ESR spectrum of PTX shows the existence of other radicals, which were not trapped by DMPO, except the DMPO radicals. This result may be addressed to the macromolecular structure of PTX. The steric hindrance of the macromolecular coil could be unfavor of the recombination between DMPO and radicals, thus some radicals could not escape from the macromolecular coil cage timely to be trapped by DMPO.

3.2.3. Photopolymerization of TMPTA

The photo-DSC profiles of the polymerization of TMPTA for two photoinitiator systems are shown in Fig. 4, which shows both photoinitator systems are effective.

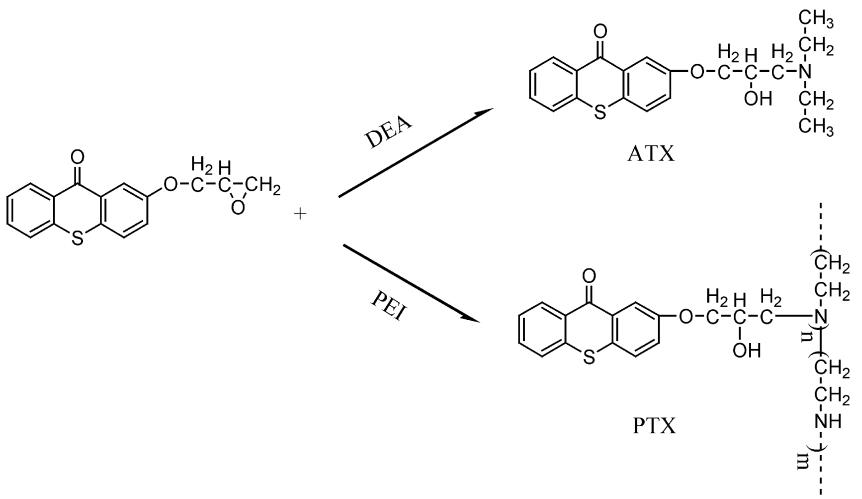

Scheme 1.

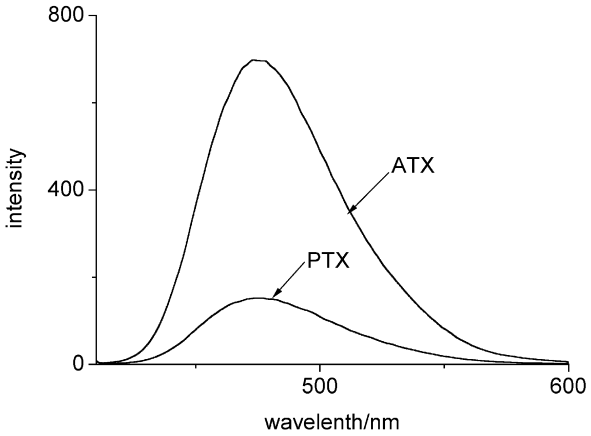

Fig. 2. Fluorescence spectra of PTX and ATX/DEA in ethanol solution, Ex = 398 nm (PTX = 1×10^{-5} M, ATX = 1×10^{-5} M).

This polymerization behavior appears similarly to other multifunctional monomers [12,14,28–31]. In the photopolymerization of multifunctional monomers, gelation often occurs at an early stage of the reaction. The formation of a three-dimensional gel structure restricts the diffusion and mobility of both macroradicals and pendant double bonds, slowing down the radical termination rate. This results in a buildup of radical species, promoting the rate of polymerization, leading to autoacceleration. However, when the reaction continues, the increased cross-linking level eventually limits the monomer mobility; the propagation reaction then also becomes diffusion controlled along with radical termination. Thus, the overall polymerization rate begins to decrease. As the mobility of the reaction system is further reduced, the reactive species become trapped, and the reaction eventually stops.

The major differences between two photopolymerization systems were that the polymerization rate of PTX was slower than that of ATX/DEA at early stage, but faster at later stage. This was obviously observed in the Fig. 5(a), which shows the relationship between the polymerization rate and the conversion for two photoinitiator systems. This result may be addressed to the macromolecular effect of PTX. At early polymerization stage, macroradicals are not as active as low-molecular-weight radicals because of the low mobility of macromolecular chains, and the difficulty of some macromolecular radicals in escaping from the cage timely to initiate the polymerization for the steric hindrance

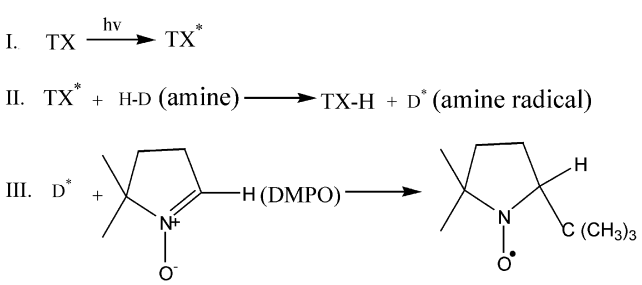

Scheme 2.

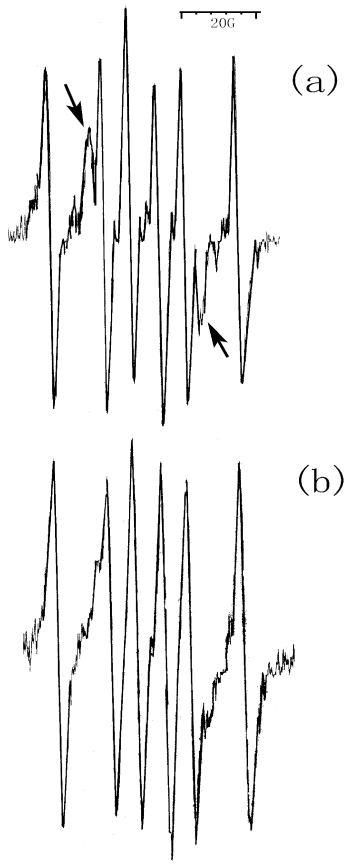

Fig. 3. ESR spectra of PTX (a) and ATX/DEA (b), photolysis time 3 min.

of the macromolecular coil (see Section 3.2.2), further more, radicals located on polymer chain for PTX could not dispersed as uniformly as in the system for ATX/DEA. As the polymerization time goes on, the number of low-molecular-weight radicals is less than that of macroradicals because of its higher termination rate. The steric hindrance of the macromolecular coil is unfavor of the recombination reactions between the propagating radicals and macroradicals, thus strongly limiting the extent of terminations and hence preventing a reduction of the concentration of the

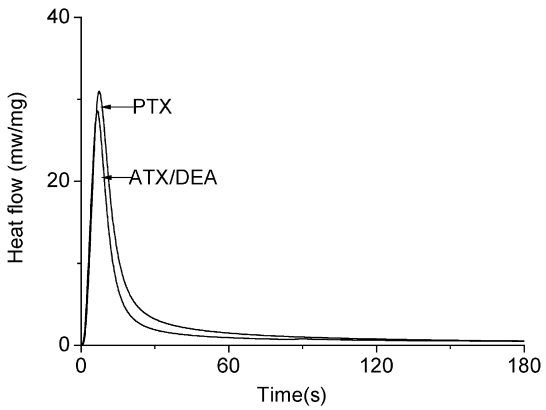

Fig. 4. Photo-DSC profiles for PTX and ATX/DEA in TMPTA, cured at 25 °C by UV light with an intensity of 50 mw/cm^2 (PTX = 0.07 M; ATX = 0.07 M).

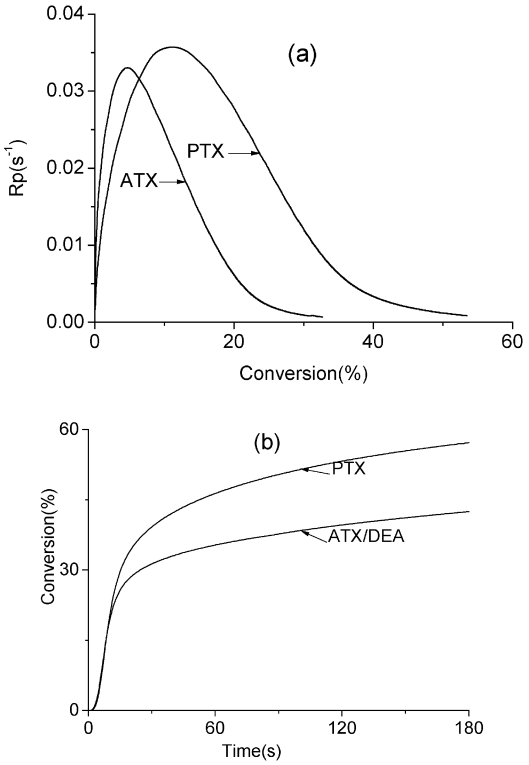

Fig. 5. (a) Rate vs. conversion; (b) conversion vs. time, for polymerization of TMPTA for PTX and ATX/DEA, cured at 25 °C by UV light with an intensity of 50 mw/cm^2 (PTX = 0.07 M; ATX = 0.07 M).

active species. Moreover, at higher conversion, the intramolecular H-abstraction between amino backbone and TX in PTX is less effected by gel effect than that in ATX/DEA because of the higher local amino concentration in PTX, which makes PTX photoinitiator systems yield more active species. Fig. 5(b) shows the relationship between the conversion and time for two photoinitiator systems. The final conversion of TMPTA for PTX system is higher than that for ATX/DEA system, which shows that PTX can carry out the photopolymerization of TMPTA more effectively.

3.3. Kinetic study of photopolymerization of TMPTA initiated by PTX

3.3.1. Influence of initiator concentration

Comparisons of the rate of isothermal photopolymerization at different PTX concentrations are presented in Fig. 6. The rate of photopolymerization can be expressed by the equation [32]

$$R_p = -\mathrm{d[M]}/\mathrm{d}t = k_p/k_t^{1/2}[\mathrm{M}](\phi\varepsilon I_0[\mathrm{A}]_0)^{1/2} \quad (3)$$

Where k_p and k_t are the propagation and termination rate constants, [M] is the molar concentration of the acrylate group, Φ is the initiation efficiency, ε is the absorption coefficient, I_0 is the incident light intensity, and [A] is the photoinitiator concentration. Fig. 6 shows that the time to reach the maximum polymerization rate decreases with

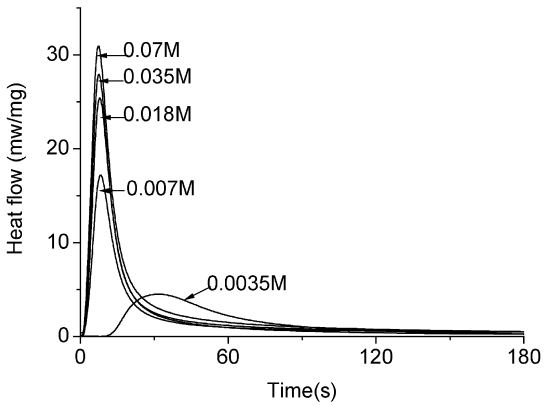

Fig. 6. Photo-DSC profiles of TMPTA for different PTX concentrations, cured at 25 °C by UV.

increased PTX concentration. Especially at the very low PTX concentration (0.0035 M), it takes more than 30 s to reach the maximum (while the others need less than 10 s). This is because that very low initiator concentration yields few radicals by the incident light, thus leads to the requirement of a long period of time to form the gel structure which produces a maximum in the polymerization rate.

Fig. 7 shows that the maximum polymerization rate occurs at higher conversion, and the final conversion

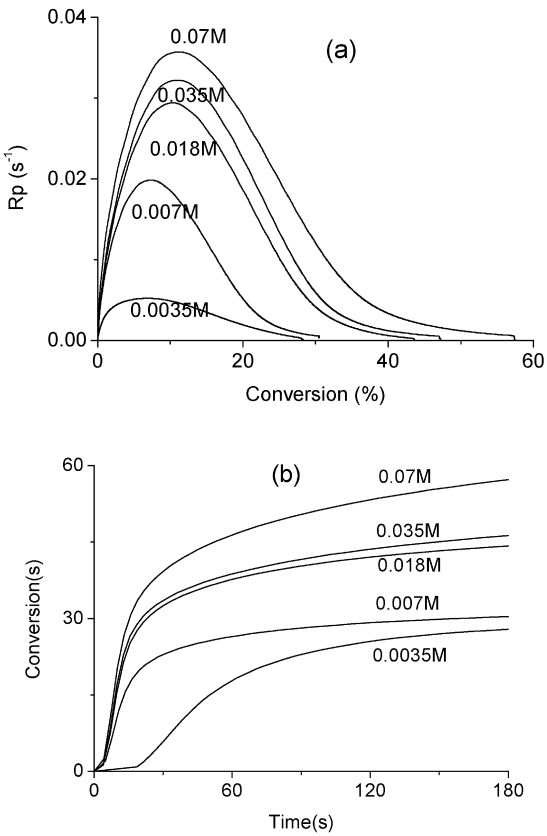

Fig. 7. (a) Rate vs. conversion; (b) conversion vs. time, for polymerization of TMPTA at different PTX concentrations, cured at 25 °C by UV light with an intensity of 50 mw/cm^2.

increases as the PTX concentration increases. This may be attributed to the free volume effect, which is caused by the delay in the volume shrinkage rate [15,31,33,34]. In the case of photoinitiated polymerization, initiation rate is very high. Thus, cross-linking systems can not be in volumic equilibrium because the volume shrinkage rate is much smaller than the chemical reaction rate. This difference generates a temporary excess of free volume which increases the mobility of the residual double-bond and leads to a higher conversion.

Conversion rate verus $[PTX]_0^{0.5}$ plots (Fig. 8) show the limitation of the Eq. (3) with a deviation from the linearity when the photoinitator concentration increases. Similar behavior has been observed in photopolymerization of the dimethacrylates [31]. This may be ascribed to the decrease of the initiation efficiency with the increase of photoinitiator concentration and preliminary radicals located on polymer chain.

3.3.2. Influence of light intensity

Figs. 9 and 10 show that the light intensity has the similar effect on the polymerization to the phototoinitiator concentration. The increase in the light intensity leads to the increase in the polymerization rate and final conversion. This similar result can be accepted according to the Eq. (3). In contrast to the deviation of linearity for conversion rate verus $[PTX]_0^{0.5}$ plots (Fig. 8), however, the initial slopes of the curves (R_p) are almost in agreement with the Eq. (3) and proportion to $I_0^{0.5}$ (Fig. 11). This shows that the light intensity has not obvious effect on initiation efficiency Φ.

3.3.3. Influence of the temperature

Fig. 12 is the photo-DSC profiles of the polymerization initiated by PTX at different temperature. It shows that the time taken to reach the exotherm peak is essentially independent of the isothermal curing temperature and that the maximum rate of photopolymerization only increases by twofold even though the polymerization temperature is raised by more than 50 °C. Scott [35] reported the similar results. This is because that the rate of decomposition of a photoinitiator is not dependent on the temperature.

Arrhenius plots of the rate data at different conversions are shown in Fig. 13. At a low conversion (10%), the Arrhenius plot is linear, and from the slope of the plot, we can obtain that the apparent activation energy is

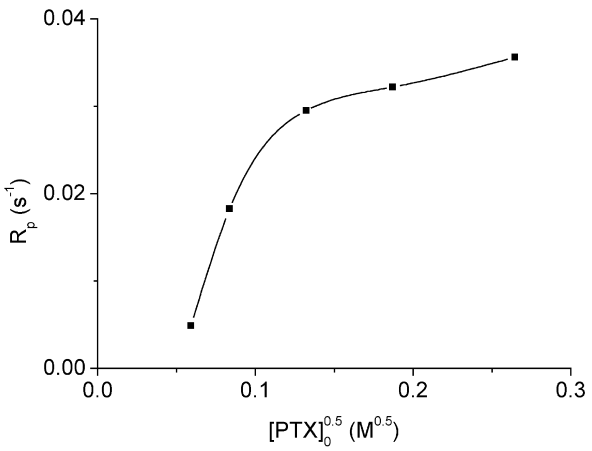

Fig. 8. Polymerization rate (at 10% conversion) vs. $[PTX]_0^{0.5}$ for TMPTA/PTX systems, cured at 25 °C by UV light with an intensity of 50 mw/cm^2.

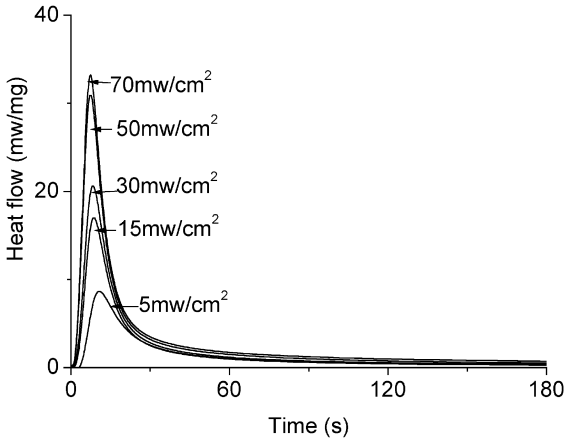

Fig. 9. Photo-DSC profiles, for polymerization of TMPTA for different light intensity, cured at 25 °C with [PTX] = 0.07 M.

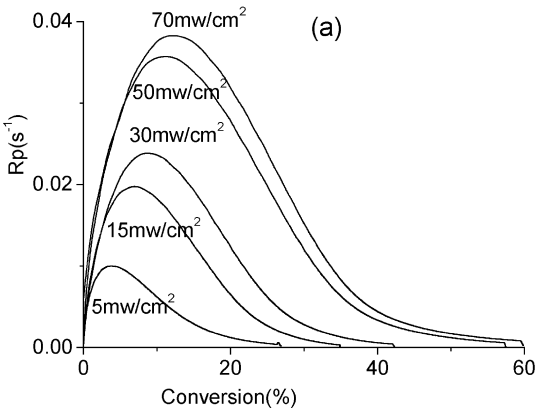

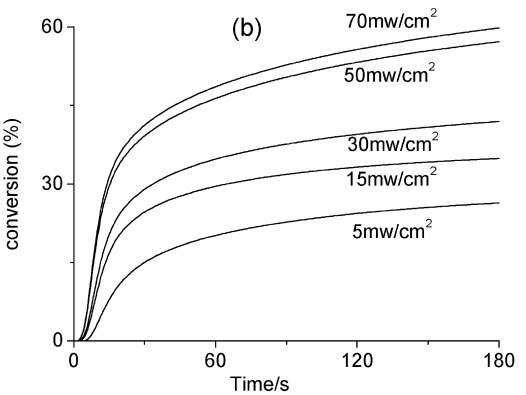

Fig. 10. (a) Rate vs. conversion; (b) conversion vs. time, for polymerization of TMPTA, for different light intensity, cured at 25 °Cwith [PTX] = 0.07 M.

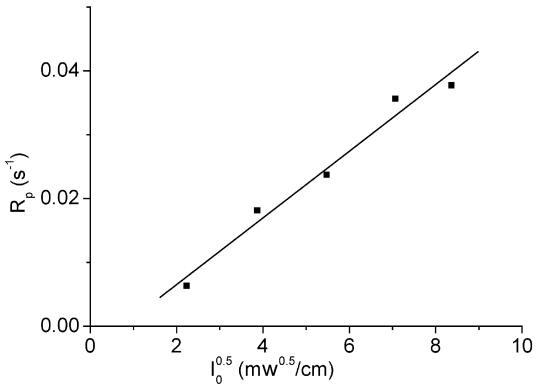

Fig. 11. Polymerization rate (at 10% conversion) vs. $I_0^{0.5}$ for TMPTA/PTX system, cured at 25 °Cwith [PTX] = 0.07 M.

6.6 kJ mol^{-1}. At a high conversion, however, the Arrhenius plot is curved. This may be due to the diffusion-controlled kinetics for the late stage of the cross-linking polymerizations. The increased cross-linking level eventually limits the molecular mobility, then the propagation and termination steps become diffusion controlled. In this case, as the molecular mobility drops with the decrease of the polymerization temperature, the reaction rate becomes markedly slower than that predicted by the Arrhenius equation.

The maximum polymerization rate of TMPTA occurs at a higher conversion as the polymerization temperature increases (see Fig. 14(a)). This behavior is in agreement with the chemico-diffusion modeling of polymerization made by Cook [12,13]. Fig. 14(b) shows that raising the isothermal cure temperature also results in increased final conversion, as has been found in other thermosetting systems [12,13,28,33,35–37]. This increase in the conversion is mainly due to the increased mobility of the reactive species. Since increasing temperature lifts the limitation of the T_g on the polymerization and makes the polymeric radicals more mobile, and the reaction systems can further polymerize and reach a higher level of conversion before the T_g of the network reaches the curing temperature.

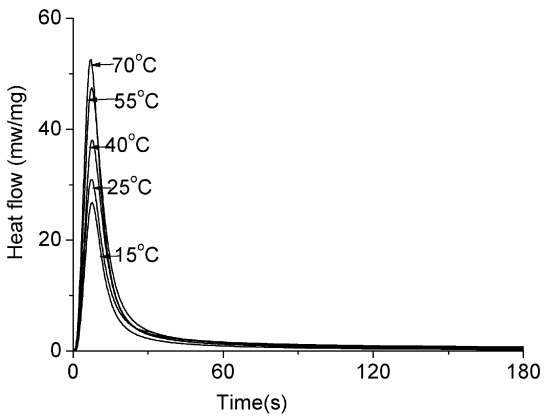

Fig. 12. Photo-DSC profiles for polymerization of TMPTA measured at different temperatures, [PTX] = 0.07 M with light intensity of 50 mw/cm^2.

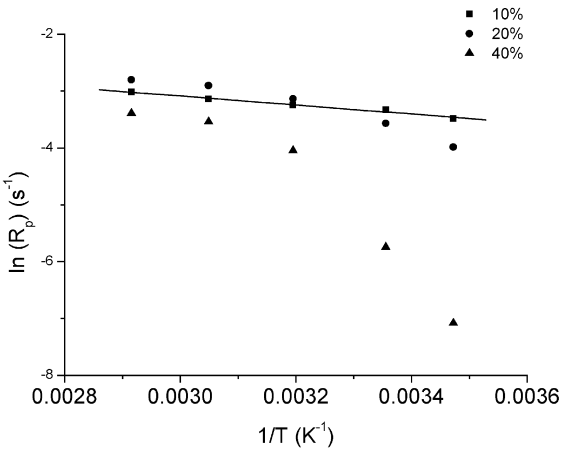

Fig. 13. Arrhenius plots of the rate at different conversions, [PTX] = 0.07 M with light intensity of 50 mw/cm^2. UV+ light with an intensity of 50 mw/cm^2.

4. Conclusions

1. Polymeric photoinitiator, prepared by covalently linking the photosensitive moiety of thioxanthone to the side chain of poly(ethylene imine), has the similar UV–vis absorption and weaker fluorescence emission compared

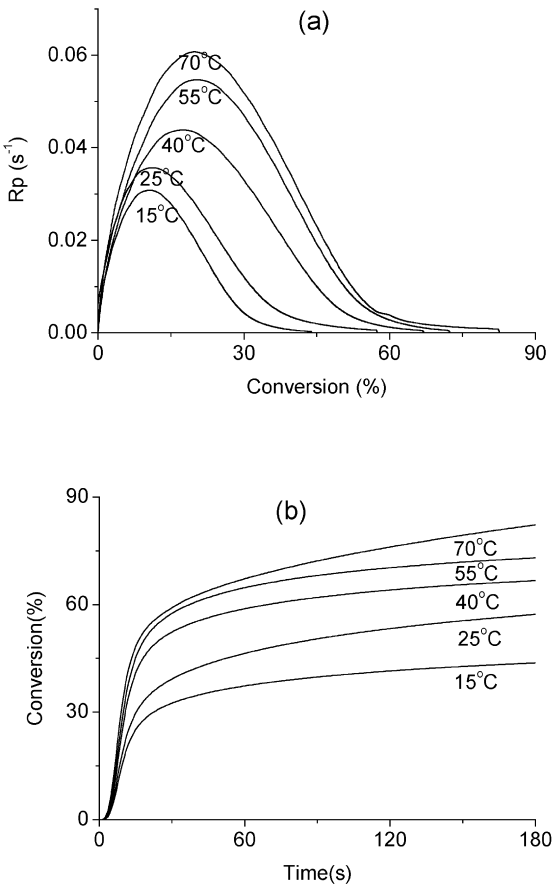

Fig. 14. (a) Rate vs. conversion, (b) conversion vs. time, for polymerization of TMPTA measured at different temperatures, [PTX] = 0.07 M with light intensity of 50 mw/cm^2.

to the corresponding small molecular photoinitiator system, and can be used to photocure TMPTA effectively with higher final conversion and polymerization rate.
2. Photoinitiator concentration and light intensity have similar effect on the polymerization process of TMPTA using PTX as photoinitiator. The increase in PTX concentration and light intensity results in the increase in the polymerization rate and the final conversion.
3. The increase in polymerization temperature leads to the increase in the polymerization rate and final conversion, due to increased molecular mobility and delay in vitrification at high temperature. At the late stage of polymerization, the reaction becomes more diffusion-controlled than that at early stage of polymerization.

Acknowledgements

The authors express their gratitude to the Ministry of Education of China (Kuashiji Scholar project and Key Young Teacher' Project) and the Science and Technology Commission of Shanghai for their financial support.

References

[1] Fouassier JP. Photoinitiation, photopolymerization, and photocuring fundamentals and applications. New York: Hanser Publishers; 1995. Chapter 1 and 6.
[2] Fouassier JP, Lougnot DJ, Avar L. Polymer 1995;36:5005.
[3] Robert L. J Polym Sci Part A: Polym Chem 2002;40:1504.
[4] Wataru T, Yuji N, Nobuyuki T, Hidenori U, Masayuki O, Yukinori N. Bimaterials 2003;24:2097.
[5] Beena G, Dhamodharan R. Polym Int 2001;50:897.
[6] Carlini C, Angiolini L, Caretti D, Corelli E. Polym Adv Technol 1996; 7:379.
[7] Angiolini L, Caretti D, Corelli E, Carlini C, Rolla PA. J Appl Polym Sci 1997;64:2247.
[8] Angiolini L, Caretti D, Salatelli E. Macromol Chem Phys 2000;201: 2646.
[9] Ajayaghosh A. Polymer 1995;36:2049.
[10] Angiolini L, Caretti D, Carlini C, Corelli E, Salatelli E. Polymer 1999; 40:7197.
[11] Decker C. Macromolol Rapid Commun 2002;23:1067.
[12] Cook WD. Polymer 1992;33:2152.
[13] Cook WD. J Polym Sci Part A: Polym Chem 1993;31:1053.
[14] Khudyakov IV, Legg JC, Purvis MB, Overton BJ. Ind Engng Chem Res 1999;38:3353.
[15] Anseth KS, Wang CM, Bowman CN. Macromolecules 1994;27:650.
[16] Peinado C, Alonso A, Salvador EF, Baselga J, Catalina F. Polymer 2002;43:5355.
[17] Scherzer T. Macromol Symp 2002;184:79.
[18] Mateo JL, Calvo M, Serrano J, Bosch P. Macromolecules 1999;32: 5243.
[19] Young JS, Kannurpatti AR, Bowman CN. Macomol Chem Phys 1998; 199:1043.
[20] Lee TY, Roper TM, Jonsson ES, Kudyakov I. Polymer 2003;44:2859.
[21] Anderson DG, Davidson RS, Elvery JJ. Polymer 1996;37:2477.
[22] Corrales T, Catalina F, Peinado C, Allen NS. Polymer 2002;43:4591.
[23] Pouliquen L, Conqueret X, Fabrice MS, Fouassier JP. Macromolecules 1989;22:108.
[24] Lougnot DJ, Tuck C, Fouassier JP. Macromolecules 1995;28:8028.
[25] Cokbaglan L, Arsu N, Yagci Y, Jackusch S. Macromolecules 2003; 36:2649.
[26] Andrejewska E, Andrzejewski M. J Polym Sci Part A: Polym Chem 1998;36:665.
[27] Yang JW, Zeng ZH, Chen YL. J Polym Sci Part A: Polym Chem 1998; 36:2563.
[28] Cook WD. Polymer 1992;33:600.
[29] Anseth KS, Wang CM, Bowman CN. Polymer 1994;35:3243.
[30] Lecamp L, Youssef B, Bunel C. Polymer 1999;40:1403.
[31] Yu Q, Nauman S, Santerre JP, Zhu S. J Appl Polym Sci 2001;82:1107.
[32] Odian G. Princinples of polymerization, 3rd ed. New York: Wiley; 1991.
[33] Lecamp L, Youssef B, Bunel C. Polymer 1997;38:6089.
[34] Bowman CN, Peppas NA. Macromolecules 1991;124:1914.
[35] Scott TF, Cook WD, Forsythe JS. Polymer 2002;43:5839.
[36] Cook WD, Simon GP, Burchill PJ, Lau M, Fitch TJ. J Appl Polym Sci 1997;64:769.
[37] Wisanrakkit G, Gillham JK. J Appl Polym Sci 1990;41:2885.